Solid-state studies into the possible rearrangement mechanisms for the fluxional behaviour of the tetranuclear carbonyls $M_4(CO)_{12}$ and their derivatives

Brian F.G. Johnson [a], Yvonne V. Roberts [a], Emilio Parisini [b] and Robert E. Benfield [c]

[a] *Department of Chemistry, The University of Edinburgh, West Mains Road, Edinburgh, EH9 3JJ (UK)*
[b] *Instituto Chimico 'G. Ciamician', Universita degli Studi di Bologna, 40126, Bologna (Italy)*
[c] *University Chemical Laboratory, University of Kent, Canterbury, CT2 7NH (UK)*

Abstract

The deformation from an idealised geometry, observed in the solid state for a given cluster species, may indicate the paths taken by the cluster in ligand fluxionality processes. A number of single-crystal X-ray structures of $M_4(CO)_{12-n}(L)_n$ clusters (M = Co, Rh, Ir; n = 1–5) have been examined in order to elucidate any geometric trends in their ligand envelope deformations. It has been revealed that the complementary geometries adopted by $M_4(CO)_{12-n}(L)_n$ species may be both metal- and ligand-dependent. Iridium species adopt T_d-cubeoctahedral structures, but the available data provide no clear picture for the complementary geometry adopted by cobalt or rhodium species. Additionally, tripodal ligands have been shown to stabilise D_{3h} (icosahedral) ligand polyhedra.

Key words: Molybdenum; Rhodium; Iridium; Crystal structure; Fluxionality; Carbonyl

1. Introduction

As for those of the $M_3(CO)_{12}$ binary carbonyls of the iron triad [1], rationalisation of the structures of $Co_4(CO)_{12}$ [2], $Rh_4(CO)_{12}$ and $Ir_4(CO)_{12}$ [3] has proved difficult. The problem arises from the observation that two distinct structural types exist for $M_4(CO)_{12}$ species: $Co_4(CO)_{12}$ and $Rh_4(CO)_{12}$ adopt an overall C_{3v} configuration with nine terminal CO ligands and three μ_2 bridges around the base-of the M_4 tetrahedron, and $Ir_4(CO)_{12}$ adopts an arrangement of T_d symmetry with three terminally-bonded CO ligands per Ir atom (Fig. 1). We have previously observed that in the cobalt and rhodium systems the carbonyl envelope forms an icosahedron, whereas for the iridium analogue the distribution is cubeoctahedral [4].

Carbonyl fluxionality has been observed for both $Co_4(CO)_{12}$ [5] and $Rh_4(CO)_{12}$ [6] but attempts to identify the exact mechanism(s) involved has led to consid-

erable controversy. Indeed, examination of the mixed metal cluster $Co_3Rh(CO)_{12}$ clearly demonstrated that no *single* mechanistic pathway could account for the complexity of the observed fluxionality [7], a point reinforced by the observation of at least three rearrangement processes for the iridium complex $Ir_4(CO)_{11}PPh_2Me$ [8]. Two early mechanisms proposed for the carbonyl migration in $M_4(CO)_{12}$ (M = Co, Rh) systems, involved *either* a D_{2d} symmetry intermediate with four μ_2 bridges [9] or simultaneous opening of the existing three μ_2 bridges to form an intermediate with a *pseudo*-$Ir_4(CO)_{12}$ structure and of T_d symmetry.

We have proposed in the past [4] that the solid-state structures and fluxional behaviour of $M_m(CO)_n$ clusters may be best explained in terms of the *Ligand Polyhedral Model* (LPM). The LPM views these clusters as either a polyhedron or polygon (the M_m unit) packed inside another [the $(CO)_n$ ligand set]. For example, two forms of $M_4(CO)_{12}$ (M = Co, Rh) with C_{3v} or T_d symmetry can arise from two different *idealised* orientations of the M_4 tetrahedron within a low energy $(CO)_{12}$ icosahedron (Fig. 2). Interconversion between
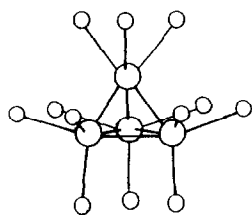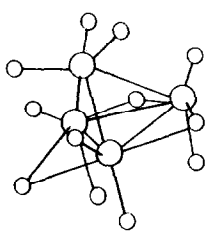

Fig. 1. The molecular structures of $Co_4(CO)_{12}$, $Rh_4(CO)_{12}$ and $Ir_4(CO)_{12}$.
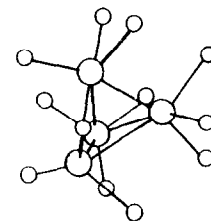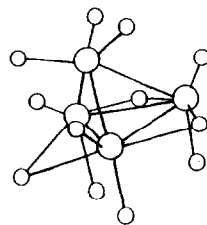

Fig. 2. Possible structures of the isomeric forms of $Co_4(CO)_{12}$ and $Rh_4(CO)_{12}$.

these two forms may be achieved by simple libration of the M_4 tetrahedron within a static CO icosahedron. In contrast, the observed solid-state structure of $Ir_4(CO)_{12}$ is the result of inserting the tetrahedral Ir_4 cluster unit into the energetically 'less favourable' cubeoctahedral arrangement of CO ligands. In this connection, it is important to recognise that although the all-terminal T_d form of $Co_4(CO)_{12}$ and the all-terminal T_d form of $Ir_4(CO)_{12}$ are very similar, consisting of four $M(CO)_3$ units bonded to form a tetrahedron, they are *not* the same. Lauher has extended this idea to form the basis of molecular mechanics calculations for these species [10], including the relative stabilities of the possible structural forms of $M_4(CO)_{12}$.

We believe libration of the M_4 tetrahedron to be a dominating feature in the solid cluster; any flexing of the CO polyhedron will be constrained by the demands of the crystallographic lattice. We have previously pointed out that this is the process that accounts most satisfactorily for the observed fluxionality in the solid, a view recently endorsed by the work of Heaton *et al.* [11] on the $Co_4(CO)_{12}$ system. However, it must be emphasised that CO equilibration *does* occur by this process, without the actual interchange of CO positions.

In solution, such crystallographic constraints are removed and genuine CO interchange may occur. We

believe that this operation is concerted and proceeds via a readily accessible transition state. Given the observed ground-state geometries of the three carbonyls $M_4(CO)_{12}$ (M = Co, Rh or Ir), it would appear that there are three readily accessible ligand polyhedra, *viz.*, the icosahedron, the cubeoctahedron and the anticubeoctahedron. Interconversion between these polyhedra would provide a method by which CO scrambling might occur.

In earlier work [4] we suggested that interconversion proceeded via a cubeoctahedral transition state. This mechanism is limited by the fact that the antipodal relationship of ligands in the icosahedral shell is sustained throughout the process; thus *total* scrambling can never occur. This is illustrated in Fig. 3. More recently we have recognised that interconversion through the alternative anticubeoctahedron does not present this problem. With this transition state *total* CO scrambling is possible (Fig. 4(a)).

We wish to emphasise that the LPM does not detract from other, accepted mechanisms for fluxional rearrangements. Indeed our proposals for icosahedral fluxionality embrace the CO-terminal ⇌ CO-bridge interchange proposed by Cotton [12]. The only difference is in our holistic approach to molecular geometry, which is analogous to that used in Berry *pseudo*-rotation, rather than the localised view employed by many of our colleagues.
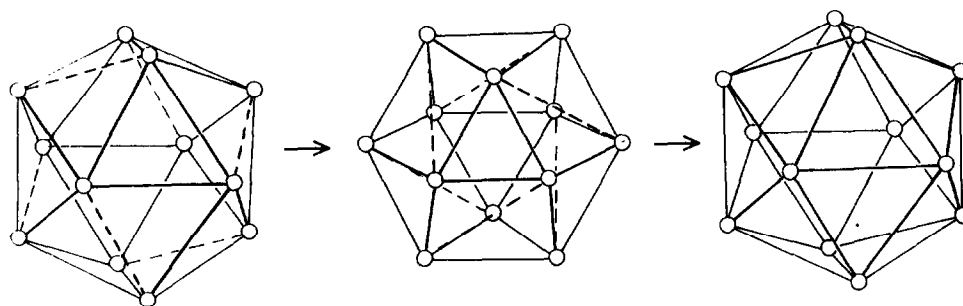

Fig. 3. Icosahedral interconversion through a cubeoctahedral transition state.
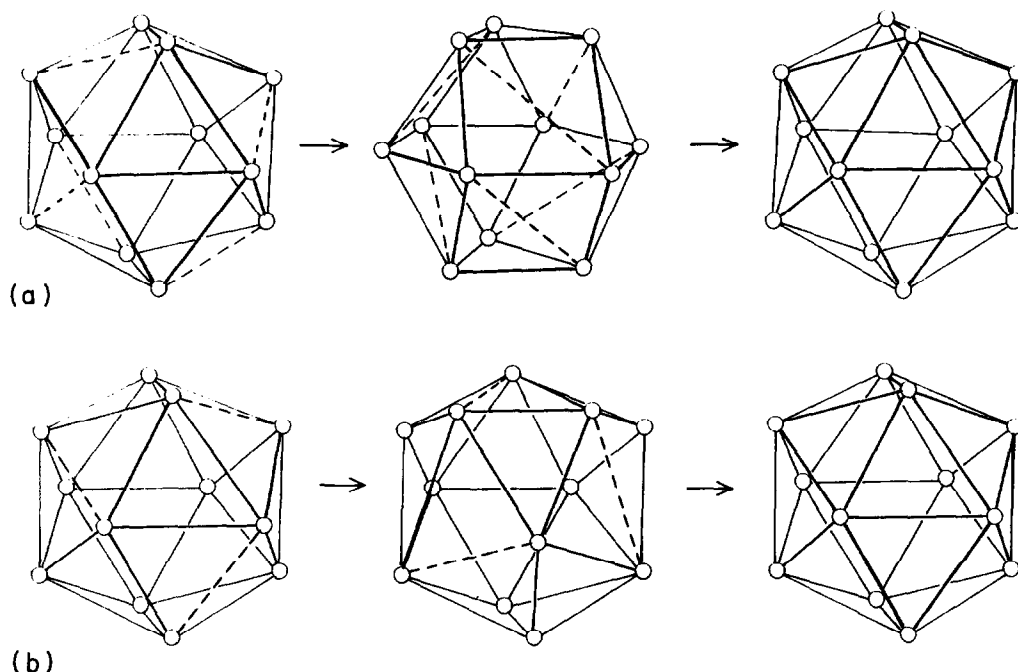
Fig. 4. (a) Icosahedral interconversion through an anticubeoctahedral transition state; (b) Icosahedral interconversion through a D_{3h}-icosahedral transition state.

Of course, the cubeoctahedron and the anticubeoctahedron are the most obvious transition states. There are other possibilities such as the D_{3h} icosahedron and the bicapped right pentagonal prism. We previously reported that a study of the crystal structures of the carbonyl clusters $M_3(CO)_{12}$ (M = Fe, Ru or Os) and a series of their derivatives $M_3(CO)_{12-n}(L)_n$ had revealed good evidence in support of the hypothesis that ligand rearrangement proceeds via the intermediacy of an anticubeoctahedral complementary geometry. No evidence for the bicapped pentagonal antiprism alternative was found. However, we had not taken into account the possibility of a D_{3h}-icosahedral ligand geometry.

In this paper we wish to present evidence for metal-specific complementary geometries for $M_4(CO)_{12}$-type species, based on the Dunitz and Bürgi approach [13]. They propose that molecular deformation in the solid state might be expected to be along vectors related to soft vibration modes. A similar analysis of terminal and bridging carbonyl bonding modes has already been investigated [14]. These same vibrational modes may also be indicative of the mechanisms employed in the observed fluxionality of $M_4(CO)_{12-n}$ $(L)_n$ species.

2. Method

Fractional coordinate data for structures 1–31 [2,3,15–43] were retrieved from the Cambridge Struc-

tural Database via the Crystal Search and Retrieval Programme at Daresbury [44]. Molecular geometry calculations utilised CALC [45] and the corresponding pictorial and graphical representations were generated using SHELXTL [46] and EASYGRAPH, respectively.

The calculated polyhedral parameters were derived from an idealised anticubeoctahedron with each vertex describing the position of an O atom or another, coordinated atom [Fig. 5(b)]. The O atom of each CO ligand was taken to describe each vertex of the outer polyhedron, in preference to the C atom. The Ru–O distances (typically 3.0 Å) are much more comparable with Ru–P distances (typically 2.4 Å), and provide a more accurate description of the polyhedron shape. No modification, for example sphericalisation of ligand positions [47], of the ligand polyhedra was undertaken. The M_4 tetrahedron is orientated such that one of its triangular faces is nearly parallel to the bottom face of the outer polyhedron. A projected view of the polyhedron from the top face [Fig. 5(a)] shows the top and bottom triangular faces of the outer polyhedron and the M_4 tetrahedron all mutually eclipsed. As distortion towards icosahedral occurs, the outer polyhedral triangular faces become rotated ($\alpha°$) with respect to each other [Fig. 5(c)] and the six shaded atoms in Fig. 5(a) deviate from planarity [Fig. 5(d)]. Similarly, the rotation angles between the projected M_4 tetrahedron and either the top ($\beta°$) of bottom ($\gamma°$) can be measured. In the most extreme case, i.e. icosahedral, the outer triangular faces are fully staggered [Fig. 5(c); $\alpha = 60°$] and
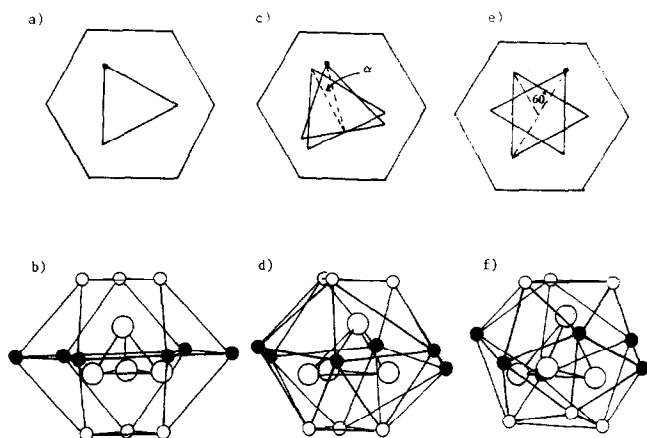
Fig. 5. Calculated polyhedral parameters for an anticubeoctahedron → icosahedron conversion.

Fig. 6. A comparison of D_{3h}-icosahedral and anticubeoctahedral geometries.

the six shaded atoms adopt the 'chair' conformation [Fig. 5(f)].

The average deviation from planarity (σ) of the six shaded atoms is calculated for the best fit plane of all six. However, exactly the same parameters, $\alpha = 0°$ and $\sigma = 0°$ are found to describe the D_{3h} icosahedron, as well as the anticubeoctahedron. Although the two shapes are visually distinguishable (see Fig. 6), we have not found a suitable, simply derived parameter which can be used to corroborate the different observed geometries.

For the conversion of a cubeoctahedron to an icosahedron there is no rotation of either the top and bottom triangular faces, only a progressive puckering of the central plane of six atoms.

Normalisation of $M_4(CO)_{12-n}(L)_n$ species, due to polyhedral distortion when CO ligands are replaced by other ligand types, means that no one plane, as described above, is necessarily parallel to another. Such normalisation is usually manifested as irregular ligand polyhedra with some edges 'missing'. These irregulari-
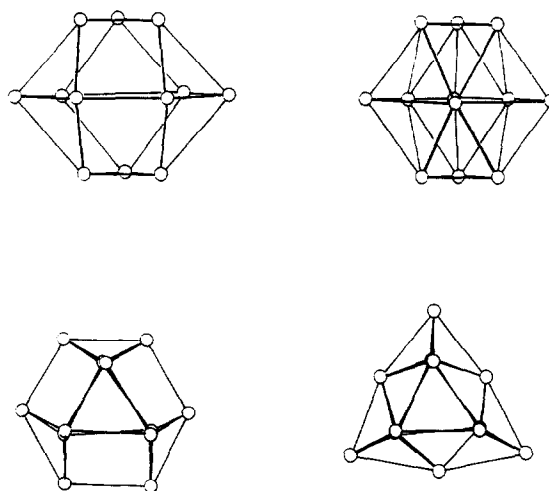
ties are quantified, in part, by the following dihedral angles:

ρ = the angle between the top and bottom outer faces;

ϕ = the angle between the top outer face and the 'base' of the M_4 triangle;

π = the angle between the bottom outer face and the 'base' of the M_4 tetrahedron;

τ = the angle between the best fit plane of the six shaded atoms and the 'base' of the M_4 tetrahedron.

3. Results and discussion

As with the previous paper [1] the structures of a wide range of cluster compounds were retrieved from the Cambridge Crystallographic database. If our sug-

TABLE 1. Polyhedral parameters [a] for $Co_{4-x}M_x(CO)_{12-n}(L)_n$ ($n = 0-5$; $x = 0, 2$; M = Rh, Ir)

Compound	α	β	γ	ρ	ϕ	π	τ	σ	Ref.
$Co_4(\mu\text{-}CO)_3(CO)_8(PMe_3)$	57.47	58.36	4.03	12.12	4.12	8.07	1.00	0.83706	15
$Co_4(\mu\text{-}CO)_3(CO)_8(PPh_3)$	50.10	57.04	7.73	3.57	2.88	6.45	1.54	0.89164	16
$Co_4(\mu\text{-}CO)_3(CO)_7[P(OMe)_3]_2$	57.69	58.77	1.34	10.94	2.15	10.51	0.49	1.67425	16
$Co_4(\mu\text{-}CO)_3(CO)_7(C_4H_3PMe_2)_2$	58.39	58.30	0.19	18.05	5.84	13.40	2.52	1.66672	17
$Co_4(\mu\text{-}CO)_3(CO)_7[(PhO)_2PN(Et)P(OPh)_2]$	56.33	55.59	0.71	6.16	3.36	8.68	0.70	0.49024	18
$Co_4(\mu\text{-}CO)_3(CO)_6[HC(PPh_2)_3] \cdot thf$	15.23	19.51	4.07	1.71	1.82	0.91	0.84	0.09581	19
$Co_4(\mu\text{-}CO)_3(CO)_5(PMe_3)[HC(PPh_2)_3] \cdot CH_2Cl_2$	14.55	9.13	5.57	3.43	3.26	0.18	0.59	0.10170	20
$Co_4(\mu\text{-}CO)_3(CO)_4(dppm)[HC(PPh_2)_3] \cdot 2MeCN$	28.34	26.30	2.51	1.84	2.38	0.91	0.43	0.39848	20
$Co_4(\mu\text{-}CO)_3(CO)_4(PMe_3)_2[HC(PPh_2)_3]$	53.51	49.33	4.32	1.68	1.57	0.95	1.63	0.43628	20
$Co_4(\mu\text{-}CO)_3(CO)_9$	58.63	55.92	5.71	8.84	3.79	5.06	2.70	1.66222	2, 26
$Co_4(CO)_8(Me_2AsCC_2F_4CAsMe_2)_2$	54.40	44.93	8.18	6.56	11.82	15.55	9.70	1.48993	21
$Co_2Ir_2(\mu\text{-}CO)_3(CO)_9$	53.01	57.67	2.69	9.17	4.12	5.36	0.81	2.22932	22
$Co_2Rh_2(\mu\text{-}CO)_3(CO)_8(PPh_3)$	56.49	57.95	1.28	3.30	2.26	5.55	1.09	2.20424	23

[a] All expressed in degrees (°).

TABLE 2. Polyhedral parameters [a] for $Rh_4(CO_{12-n}(L)_n$ ($n = 0-4$).

Compound	α	β	γ	ρ	ϕ	π	τ	σ	Ref.
$Rh_4(\mu-CO)_3(CO)_9$	57.34	55.01	7.60	4.74	2.81	2.15	2.04	1.73653	2
$Rh_4(\mu-CO)_3(CO)_8[P(^iPr)_3]$	54.56	56.52	2.11	7.42	1.37	8.69	0.79	0.79413	24
$Rh_4(\mu-CO)_3(CO)_7(PPh_3)_2$	57.81	58.43	3.18	14.29	5.50	9.71	1.91	1.46577	25
$Rh_4(\mu-CO)_3(CO)_6[P(OPh)_3]_3 \cdot thf$	54.31	57.61	2.78	14.84	4.22	12.01	4.03	1.24307	25
$Rh_4(\mu-CO)_3(CO)_5(dppm)_2$	33.01	34.59	7.64	5.41	6.05	4.80	3.73	0.39910	26
$Rh_4(\mu-CO)_4(CO)_4[HC(PPh_2)_3][P(OEt)_3] \cdot CH_2Cl_2$	2.28	1.06	3.76	17.10	18.05	1.23	4.67	0.03858	27
$Rh_4(\mu-CO)_4(CO)_5([6]aneS_3)$	5.51	5.72	0.03	21.25	21.49	0.39	3.57	0.29398	28

[a] All expressed in degrees (°).

gestions for the mechanism of ligand fluxionality are correct, then we should see some structures with an icosahedral distribution of ligands (of either C_{3v} or T_d symmetry), some structures with a cubeoctahedral (T_d) or anticubeoctahedral ligand (C_{3v}) distribution and, most importantly, structures along the pathway between the two extremes. Analysis of the atomic displacement thermal parameters (adps) showed that the Co_4 unit of $Co_4(CO)_{12}$ moves preferentially about a C_2 (rather than a C_3) axis for the $C_{3v}-T_d$ interconversion [41]. This would lead to a D_{2d} structure with four μ_2 bridges. Our studies might also provide support for this process and for the subsequent $D_{2d}-T_d$ transition.

The calculated results of these studies, as outlined above in the Method sections, are presented in tabulated form (Tables 1–3). In order to illustrate the changes in ligand polyhedral geometry actually taking place, a graphical plot of the rotation angle α against the standard deviation σ was made (see Method sec-

tion for full definitions). For a single, smooth transition, we would expect a straight line relationship in going from either anticubeoctahedral or cubeoctahedral to icosahedral. A distinctly non-linear relationship would indicate a multi-stage process.

The results are a little unexpected (see Fig. 7). Not only does the complementary geometry of a $M_4(CO)_{12-n}(L)_n$ species appear to be metal-dependent, it also appears to be linked to ligand types. The Ir_4 species make a relatively smooth transition from cubeoctahedral to icosahedral ligand envelopes, with the notable exceptions of $Ir_4(\mu-CO)_3(CO)_5(dppm)_2$ [33] and one isomer of $Ir_4(CO)_9([6]aneS_3)$ [38]. However, for the Co_4 and Rh_4 species the complementary geometry is D_{3h}-icosahedral, not the expected anticubeoctahedral form (Fig. 8). At this point a qualifier should be added: all the D_{3h}-icosahedral species $Co_4(CO)_9$-$[HC(PPh_2)_3]$ [19], $Co_4(CO)_8(PMe_3)[HC(PPh_2)_3]$ [20], $Co_4(CO)_7(dppm)[HC(PPh_2)_3]$ [20], $Rh_4(CO)_8[P(Ott)_3]$-

TABLE 3. Polyhedral parameters [a] for $Ir_4(CO)_{12-n}(L)_n$ ($n = 0-4$)

Compound	α	β	γ	ρ	ϕ	π	τ	σ	Ref.
$Ir_4(CO)_{11}(CN^tBu)$	59.90	59.72	0.20	0.93	1.89	1.60	0.69	0.02207	29
$Ir_4(CO)_{10}[1,2-(Me_2As)_2Ph]$	59.98	59.98	0.00	12.40	2.71	9.69	3.64	1.17807	30
$Ir_4(\mu-CO)_3(CO)_5(PMe_3)_4$	59.46	58.05	2.72	15.64	4.46	11.19	1.32	1.90141	31
$Ir_4(\mu-CO)_3(CO)_5(PMe_2Ph)_4$	57.26	59.96	3.11	9.15	1.42	8.79	0.64	1.46669	32
$Ir_4(\mu-CO)_3(CO)_5(dppm)_2$	29.55	26.29	6.60	3.89	4.92	4.76	2.71	1.01244	33
$Ir_4(\mu-CO)_3(CO)_5(Ph_2PCH=CHPPh_2)_2$	53.75	50.60	2.84	6.66	8.46	8.64	4.13	1.00512	34
$Ir_4(\mu-CO)_3(CO)_7(dmpe)$	55.48	55.62	0.08	7.47	3.42	8.00	1.76	1.67854	35
$Ir_4(CO)_{12}$	58.98	59.22	1.77	2.00	1.52	1.05	3.17	0.08415	3
$Ir_4(\mu-CO)_2(CO)_9(\mu-SO_2)$	55.79	56.44	7.75	4.06	2.54	2.24	0.40	1.71308	36
$Ir_4(\mu-CO)_3(CO)_7(PPh_3)_2$	58.34	55.96	0.21	13.67	5.34	9.40	1.73	1.40308	37
$Ir_4(CO)_9([6]aneS_3)$	56.88	56.57	0.78	3.24	3.06	0.18	1.84	0.14476	38
Molecule 2	56.31	56.30	0.07	3.80	4.38	0.60	0.72	0.11699	38
$Ir_4(\mu-CO)_3(CO)_6([6]aneS_3)$	42.62	43.84	1.22	5.46	5.19	0.40	0.57	0.75897	38
$Ir_4(\mu-CO)_3(CO)_7(diop)$	49.17	54.26	4.88	11.97	5.96	7.71	0.68	2.14311	39
$Ir_4(\mu-CO)_3(CO)_8(P-Clus)$ [b]	55.80	53.53	1.53	14.80	5.76	9.37	0.41	1.87756	40
$Ir_4(\mu-CO)_3(CO)_7(dppb)$	59.15	59.68	0.52	14.68	3.86	12.24	0.87	1.53523	41
$Ir_4(\mu-CO)_3(CO)_8(PPh_2AuPPh_3)$	53.08	57.13	4.24	6.98	0.90	7.79	1.35	1.75190	42
$Ir_4(CO)_9[(PPh_2)_3CH]$	53.73	58.46	7.39	2.09	1.65	0.47	0.97	0.31060	43
Molecule 2	47.10	54.22	8.06	3.18	3.13	0.49	0.40	0.30358	43

[a] All expressed in degrees (°).
[b] (P–Clus) = $PPh-PPhIr_4(CO)_9(AuPEt_3)_2$.
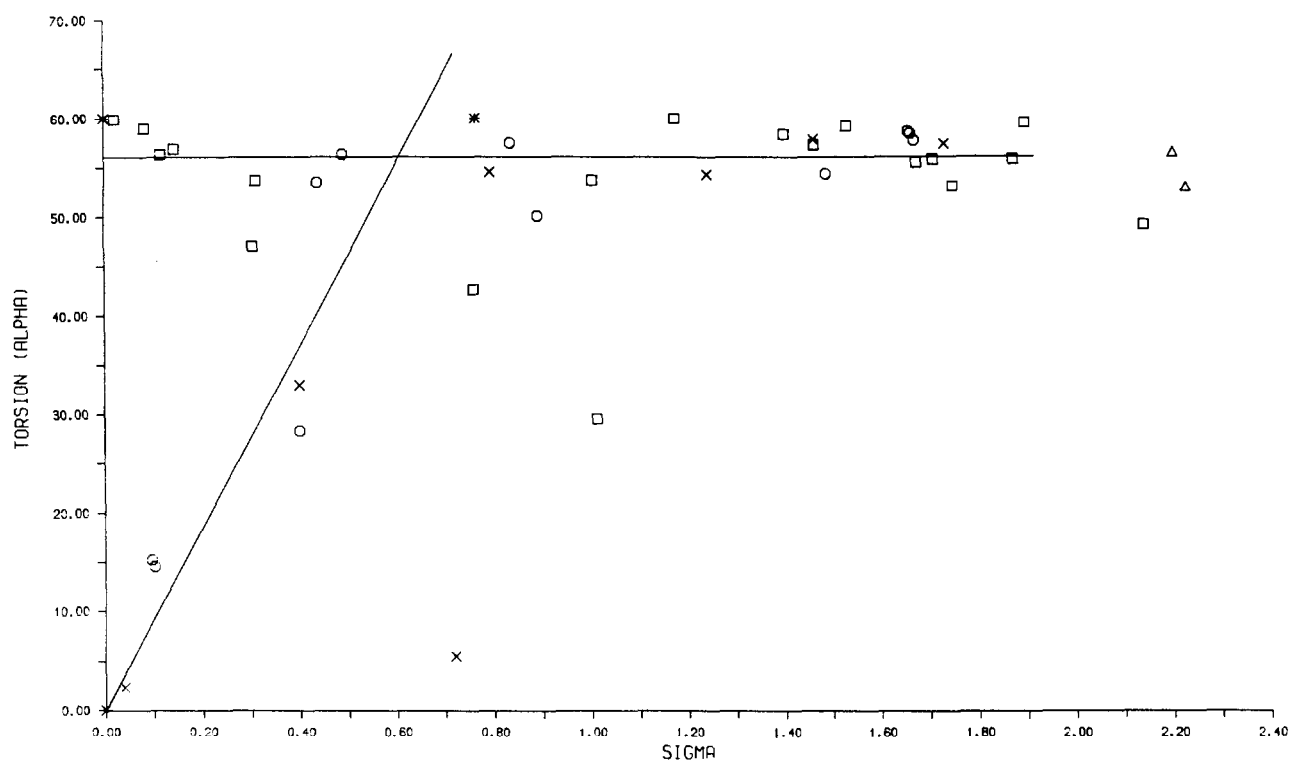
Fig. 7. Distortions to and from icosahedral ligand arrangements in compounds of the type $M_4(CO)_{12-n}(L)_n$.

[HC(PPh$_2$)$_3$] [27] and Rh$_4$(CO)$_9$([6]aneS$_3$) [28] contain a tridentate capping ligand of limited flexibility. The species Co$_4(\mu$-CO)$_3$(CO)$_4$(PMe$_3$)$_2$[HC(PPh$_2$)$_3$] [20] sits at the crossroads of the icos ↔ D_{3h}-icos transformation, being neither one thing nor the other.

Surprisingly, the Co$_4$ and Rh$_4$ D_{3h} icosahedral species are not isostructural. All the Co$_4$ complexes have three bridging carbonyls (Fig. 9), whereas the Rh$_4$ complexes have four (Fig. 10). We do not know why this should be.

In general, and as expected, the icosahedral ligand polyhedron is the most frequently observed in the structures of compounds studied to date. As predicted in an earlier report [9] substitution of carbonyl ligands by bulkier ligands such as tertiary phosphines or phosphites generally causes the ligand polyhedron to move from its parent geometry towards the appropriate complementary geometry.

Examination of the distribution of points in Fig. 7 reveals that three of the points are clearly off the intended pathways. These correspond to the species Ir$_4(\mu$-CO)$_3$(CO)$_5$(dppm)$_2$, the bridged isomer of Ir$_4$(CO)$_9$([6]aneS$_3$) and Rh$_4(\mu$-CO)$_4$(CO)$_5$([6]aneS$_3$). The distortion of the dppm complexes is understandable; the ligand envelope must be large enough to accommodate the Ir$_4$ unit, and the span of the bidentate phosphine is very small. The equivalent tetraphos-

phine species, Ir$_4(\mu$-CO)$_3$(CO)$_5$(PMe$_3$)$_4$ [30] is clearly icosahedral. However, the strong distortions caused by [6]aneS$_3$ in both the Rh$_4$ and Ir$_4$ complexes are very interesting, especially as the alternative isomer of
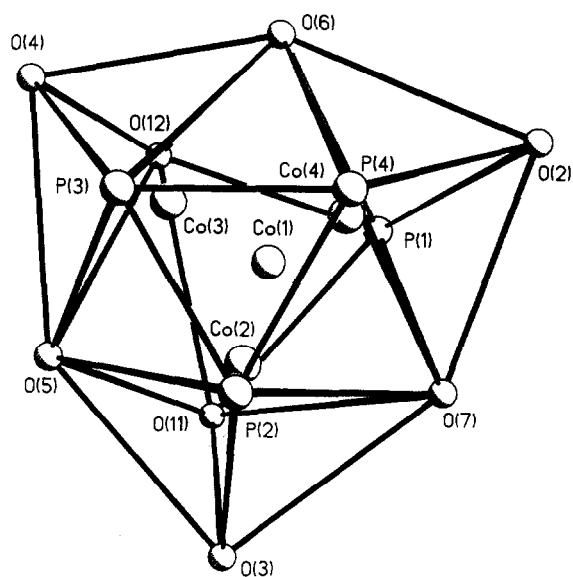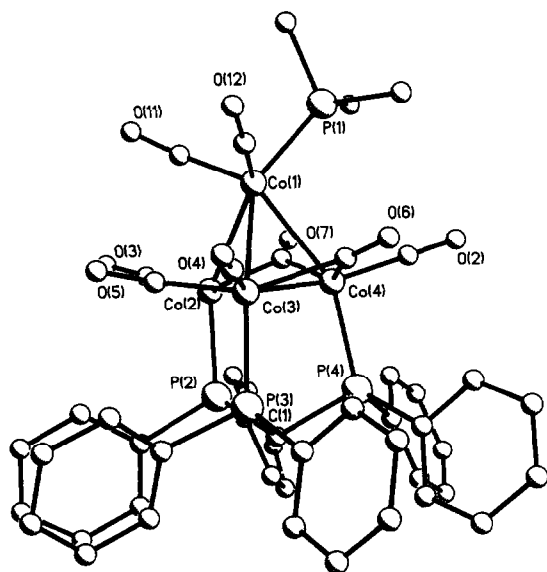

Fig. 8. An example of a D_{3h}-icosahedral polyhedron, Co$_4$(CO)$_8$-(PMe$_3$)[HC(PPh$_2$)$_3$].

Fig. 9. Alternative view of Co(CO)(PMe₃)[HC(PPh₂)₃].

Ir₄(CO)₉([6]aneS₃) [38] shows two independent *cubeoctahedral* moieties. In the iridium complex the deformation is confined to the ligand envelope, whereas in the rhodium species the central M₄ core is distorted away from tetrahedral. We have no explanation to date.

We cannot entirely rule out the anticubeoctahedron as an appropriate complementary geometry for CO₄ and Rh₄ systems, as there are no suitable crystal structures with monodentate ligands to use as a comparison. Frustratingly, the highly substituted M₄ species for
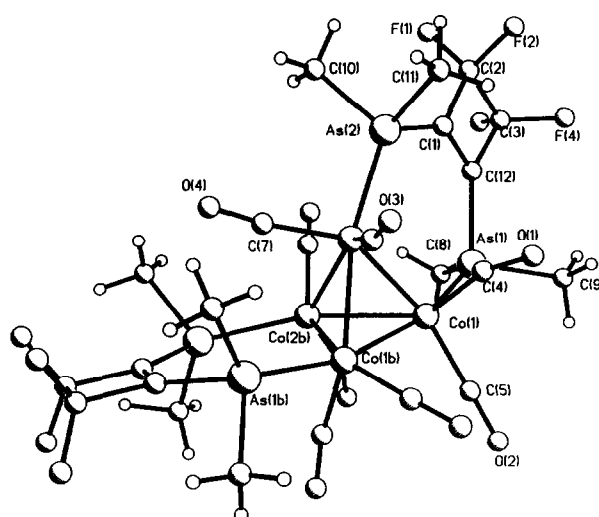
Fig. 11. All-terminal structure of Co₄(CO)₈(Me₂AsCC₂F₄CAsMe₂)₂.

which crystal structures are available are generally not the species whose fluxionality has been extensively researched and vice versa. We did not have this problem with M₃ species [1].

There is one other structure which is of particular interest. The ligands of Co₄(CO)₈(Me₂AsCC₂F₄CAs-Me₂)₂ [21] adopt an icosahedral geometry but, on closer inspection, they are found to be in an all-terminal arrangement (see Fig. 11). The symmetry is not T_d or C_{3v}, but quasi-T. This symmetry corresponds to the global minimum, calculated by Lauher, for M₄(CO)₁₂ species [10]. Lauher did not consider the possibility of

(a)   (b)
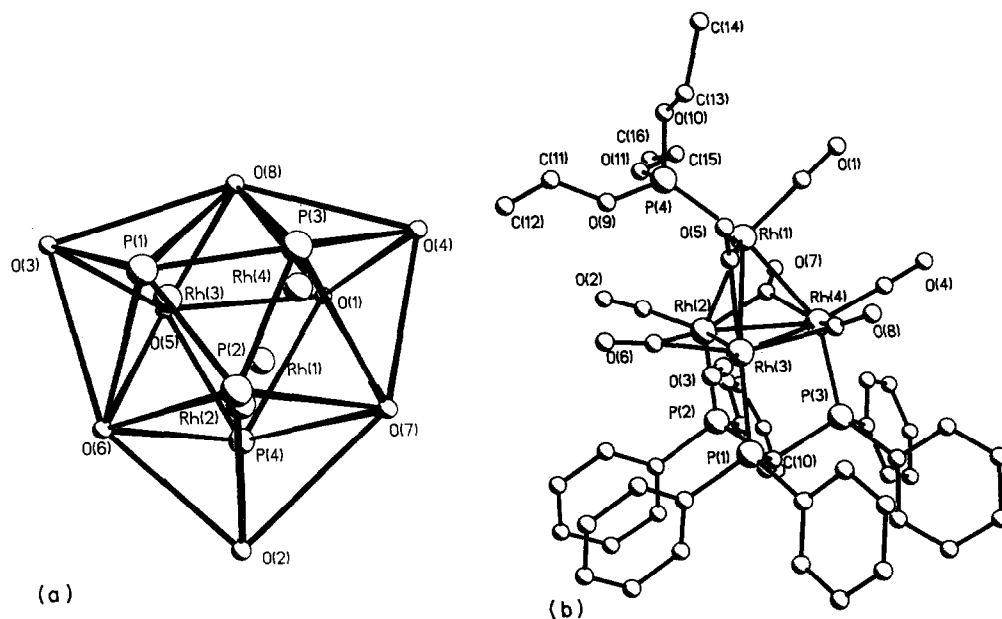
Fig. 10. Comparison views of Rh₄(CO)₈[P(OEt)₃[HC(PPh₂)₃]: (a) polyhedral; (b) structural.

anticubeoctahedral or D_{3h}-icosahedral geometries, but reported that the cubeoctahedral T_d isomer would be less stable than the icosahedral C_{3v} and T isomers. He did, however, point out that the need to attain favourable metal–metal interactions may bring about less favourable distributions of carbonyl ligands.

In conclusion, we have observed that the complementary geometry for a given $M_4(CO)_{12-n}(L)_n$ species is metal-dependent, and may also be ligand-dependent. Iridium species transmute from cubeocahedral to quasi-C_{3v} icosahedral. Cobalt and rhodium species adopt the unusual quasi-d_{3h}-icosahedral conformation when the ligand set contains a capping tridentate ligand. The cobalt and rhodium species are not isostructural, the number of carbonyl bridges is three for Co$_4$ moietes and four for Rh$_4$ species.

References

1 For a detailed description, see B.F.G. Johnson, Y.V. Roberts and E. Parisini, *J. Chem. Soc., Dalton Trans.*, (1992) 2573.
2 C.-H. Wei, *Inorg. Chem.*, 8 (1969) 2384.
3 M.R. Churchill and J.P. Hutchinson, *Inorg. Chem.*, 17 (1978) 3528.
4 B.F.G. Johnson, *J. Chem. Soc., Chem. Commun.*, (1976) 211; B.F.G. Johnson and R.E. Benfield, *J. Chem. Soc., Dalton Trans.*, (1978) 1554; R.E. Benfield and B.F.G. Johnson, *J. Chem. Soc., Dalton Trans.*, (1980) 1743.
5 J. Evans, B.F.G. Johnson, J. Lewis and T.W. Matheson, *J. Am. Chem. Soc.*, 97 (1975) 1245.
6 (a) J. Evans, B.F.G. Johnson, J. Lewis and J.R. Norton, *J. Chem. Soc., Chem. Commun.*, (1973) 807; (b) F.A. Cotton, L. Kruxzynski, B.L. Shapiro and L.F. Johnson, *J. Am. Chem. Soc.*, 94 (1972) 6191.
7 B.F.G. Johnson, J. Lewis and T.W. Matheson, *J. Chem. Soc., Chem. Commun.*, (1974) 441.
8 G.F. Stuntz and J.R. Shapley, *J. Am. Chem. Soc.*, 99 (1977) 607.
9 For a detailed description, see ref. 5.
10 J.W. Lauher, *J. Am. Chem Soc.*, 108 (1986) 1521.
11 B.T. Heaton, J. Sabounchei, S. Kernaghan, H. Nakayama, T. Eguchi, S. Takeda, N. Nakamura and H. Chihara, *Bull. Chem. Soc. Jpn.*, 63 (1990) 309.
12 F.A. Cotton, *Inorg. Chem.*, 5 (1966) 1083.
13 (a) H.-B. Bürgi, *Angew. Chem.*, 87 (1975) 461; *Angew. Chem., Int. Ed. Engl.*, 14 (1975) 460; (b) J.D. Dunitz and H.-B. Bürgi, *Acc. Chem. Res.*, 16 (1983) 153.
14 R.H. Crabtree and M. Lavin, *Inorg. Chem.*, 25 (1986) 805.
15 K. Bartl, R. Boese and G. Schmid, *J. Organomet. Chem.*, 206 (1981) 331.
16 D.J. Darensbourg, M.J. Incorvia, *Inorg. Chem.*, 20 (1981) 1911.

17 E. Keller and H. Varenkamp, *Chem. Ber.*, 114 (1981) 1111.
18 N.J. Bailey, G. De Leeuw, J.S. Field, R.J. Haines and I.C.D. Stuckenberg, *S. Afr. J. Chem.*, 38 (1985) 139.
19 D.J. Darensbourg, D.J. Zalewski and T. Delord, *Organometallics*, 3 (1984) 1210.
20 D.J. Darensbourg, D.J. Zalewski, A.L. Rheingold and R.L. Durney, *Inorg. Chem.*, 25 (1986) 3281.
21 J.W.B. Einstein, R.D.G. Jones, *J. Chem. Soc. A*, (1971) 3359.
22 V.G. Albano, G. Ciani and S. Martinengo, *J. Organomet. Chem.*, 78 (1974) 265.
23 M. Bojczuk, B.T. Heaton, S. Johnson, C.A. Ghilardi and A. Orlandini, *J. Organomet. Chem.*, 341 (1988) 473.
24 S. Maginn, *Acta Crystallogr. Sect. C*, 46 (1990) 576.
25 B.T. Heaton, L. Longhetti, D.M.P. Mingos, C.E. Briant, P.C. Minshall, B.R.C. Theobald, L. Garlaschelli and U. Sartorelli, *J. Organomet. Chem.*, 213 (1981) 333.
26 F.H. Carre, F.A. Cotton and B.A. Frenz, *Inorg. Chem.*, 15 (1976) 380.
27 J.R. Kennedy, P. Selz, A.L. Rheingold, W.C. Trogler and F. Basolo, *J. Am. Chem. Soc.*, 111 (1989) 3615.
28 R.J. Crowte, J. Evans and M. Webster, *J. Chem. Soc., Chem. Commun.*, (1984) 1344.
29 M.R. Churchill and J.P. Hutchinson, *Inorg. Chem.*, 18 (1979) 2451.
30 M.R. Churchill and J.P. Hutchinson, *Inorg. Chem.*, 19 (1980) 2765.
31 D.J. Darensbourg and B.J. Baldwin-Zuschke, *Inorg. Chem.*, 20 (1981) 3846.
32 A.J. Blake and A.G. Osborne, *J. Organomet. Chem.*, 260 (1984) 227.
33 M.M. Harding, B.S. Nicholls and A.K. Smith, *Acta Crystallogr., Sect. C*, 40 (1984) 790.
34 V.G. Albano, D. Braga, R. Ros and A. Scrivanti, *J. Chem. Soc., Chem. Commun.*, (1985) 866.
35 R. Ros, A. Scrivanti, V.G. Albano, D. Braga and L. Garlaschelli, *J. Chem. Soc., Dalton Trans.*, (1986) 2411.
36 D. Braga, R. Ros and R. Roulet, *J. Organomet. Chem.*, 286 (1985) C8.
37 U. Florke and H.-J. Haupt, *Z. Kristallogr.*, 191 (1990) 149.
38 G. Suardi, A. Strawczynski, R. Ros, R. Roulet, F. Grepioni and D. Braga, *Helv. Chim. Acta*, 73 (1990) 154.
39 D.T. Traqin, D. Dwif, M.N. Eddine, J. Leito, J.J. Rafalko and B.C. Gates, *Acta Crystallogr., Sect. B*, 38 (1982) 1916.
40 J.N. Nicholls, P.R. Raithby and M.D. Vargas, *J. Chem. Soc., Chem. Commun.*, (1986) 1617.
41 J. Strawczynski, R. Ros, R. Roulet, D. Braga, C. Gradella and F. Grepioni, *Inorg. Chim. Acta*, 170 (1990) 17.
42 D. Braga, F. Grepioni, F.S. Livotto and M.D. Vargas, *J. Organomet. Chem.*, 391 (1990) C28.
43 F.A. Clucas, M.M. Harding, B.S. Nicholls and A.K. Smith, *J. Chem. Soc., Chem. Commun.*, (1984) 319.
44 F.H. Allen, O. Kennard and R. Taylor, *Acc. Chem. Res.*, 16 (1983) 146.
45 R.O. Gould and P. Taylor, CALC, The University of Edinburgh, 1985.
46 G.M. Sheldrick, SHELXTL, P.C. Version 4.2, University of Göttingen, Germany, 1990; Siemens Analytical X-ray Instrumentation Inc., Madison, WI, USA.
47 D. Braga, C.E. Anson, A. Bott, B.F.G. Johnson and E. Marseglia, *J. Chem. Soc., Dalton Trans.*, (1990) 3517.